OXFORD

SOT | Society of Toxicology
www.toxsci.oxfordjournals.org

TOXICOLOGICAL SCIENCES, 169(2), 2019, 465–474

doi: 10.1093/toxsci/kfz060
Advance Access Publication Date: March 5, 2019
Research Article

Novel Brain-Penetrating Oxime Acetylcholinesterase Reactivators Attenuate Organophosphate-Induced Neuropathology in the Rat Hippocampus

Mary B. Dail,* Charles A. Leach,* Edward C. Meek,* Alicia K. Olivier,† Ronald B. Pringle,* Carol E. Green,‡ and Janice E. Chambers*[1]

*Department of Basic Sciences, Center for Environmental Health Sciences; †Department of Pathobiology and Population Medicine, College of Veterinary Medicine, Mississippi State University, Mississippi State, Mississippi 39762; and ‡Biosciences Division, SRI International, Menlo Park, California 94025

[1]To whom correspondence should be addressed at Basic Sciences Department, College of Veterinary Medicine, Center for Environmental Health Sciences, Mississippi State University, 240 Wise Center Drive, PO Box 6100, Mississippi State, MS. 39762-6100. Fax: (662) 325-1650; E-mail: chambers@cvm.msstate.edu.

ABSTRACT

Organophosphate (OP) anticholinesterases cause excess acetylcholine leading to seizures which, if prolonged, result in neuronal damage in the rodent brain. Novel substituted phenoxyalkyl pyridinium oximes have previously shown evidence of penetrating the rat blood-brain barrier (BBB) in *in vivo* tests with a sarin surrogate (nitrophenyl isopropyl methylphosphonate, NIMP) or the active metabolite of the insecticide parathion, paraoxon (PXN), by reducing the time to cessation of seizure-like behaviors and accumulation of glial fibrillary acidic protein, whereas 2-PAM did not. The neuroprotective ability of our lead oximes (15, 20, and 55) was tested using NeuN, Nissl, and Fluoro-Jade B staining in the rat hippocampus. Following lethal-level subcutaneous challenge with NIMP or PXN, rats were intramuscularly administered a novel oxime or 2-PAM plus atropine and euthanized at 4 days. There were statistically significant increases in the median damage scores of the NeuN-stained NIMP, NIMP/2-PAM, and NIMP/Oxime 15 groups compared with the control whereas the scores of the NIMP/Oxime 20 and NIMP/Oxime 55 were not significantly different from the control. The same pattern of statistical significance was observed with PXN. Nissl staining provided a similar pattern, but without statistical differences. Fluoro-Jade B indicated neuroprotection from PXN with novel oximes but not with 2-PAM. The longer blood residence times of Oximes 20 and 55 compared with Oxime 15 might have contributed to their greater efficacy. These results suggest that novel oximes 20 and 55 were able to penetrate the BBB and attenuate neuronal damage after NIMP and PXN exposure, indicating potential broad-spectrum usefulness.

Key words: organophosphate; acetylcholinesterase inhibitors; neuroprotection; oxime reactivators; neuropathology.

Organophosphates (OP) consist of a diverse group of compounds having a variety of uses including pesticides and chemical warfare agents (CWAs). OP insecticide poisoning has killed 5 million people during the last 30 years and continues to kill at the rate of 200,000 per year, mostly by suicide attempts (Eddleston and Chowdhury, 2016). In addition, OP nerve agents continue to threaten civilians and warfighters. The OP nerve agent, sarin, was manufactured and released by a Japanese cult in 1994 and 1995 in attacks that resulted in 19 deaths and 6,100 exposures. Up to 5 years later, EEG abnormalities were still present and many of the victims experienced post-traumatic stress disorder (PTSD) (Yanagisawa *et al.*, 2006). VX, another CWA, was used to assassinate the half-brother of North Korean leader Kim Jong Un (Swenson, 2017). The Assad regime deployed sarin in Syria in 2013 and 2017 resulting in many civilian deaths (Loveluck, 2017). More recently, Novichok, an extremely toxic OP nerve agent, was used in the March 4, 2018, attempted assassination of a former Russian spy and his daughter (Hay, 2018).

OPs are potent anticholinesterases that phosphylate acetylcholinesterase (AChE) inhibiting its ability to hydrolyze the neurotransmitter acetylcholine (ACh). This leads to an excess of ACh in synapses and neuromuscular junctions, affecting ACh receptors both in the peripheral and central nervous systems (CNS). These supraphysiological levels of cholinergic stimulation produce an array of toxic signs in exposed individuals including: muscle contractions, respiratory suppression, seizures (through glutamate excitotoxicity), and death (in instances of high level exposures) (Watson *et al.*, 2009). Despite this pressing need, little improvement in treatment has occurred. The primary antidotes for use by the United States today continue to be those of the 1950s: atropine and pralidoxime (2-PAM) (Eddleston and Chowdhury, 2016).

The antagonist atropine has reasonable CNS penetration and counteracts many of the effects of OP-induced excessive ACh by blocking cholinergic receptors both centrally and peripherally, but it does not restore the AChE activity. An oxime, such as 2-PAM, can reactivate inhibited AChE, but 2-PAM, being positively charged because of the quaternary nitrogen in its pyridine ring, does not penetrate the blood-brain barrier (BBB) to a significant enough level to restore brain AChE (Sakurada *et al.*, 2003). The cholinergic hyperexcitability leads to glutamate-mediated excitotoxicity resulting in seizures and, if prolonged and recurrent, long-term neurological impairments (Chen, 2012; Loh *et al.*, 2010). Diazepam anticonvulsant treatment fails to prevent neuronal degeneration and loss (Aroniadou-Anderjaska *et al.*, 2016).

An oxime that could cross the BBB and reactivate AChE in the CNS could both increase survival and prevent or attenuate seizures with their resulting neuropathology. For this reason, several thousand new oximes have been synthesized since the 1950s (Worek *et al.*, 2016) including our laboratory's platform of substituted phenoxyalkyl pyridinium oximes (U.S. patent 9, 227, 937) (Figure 1). Some of our novel oximes have provided convincing evidence of penetrating the rat brain in *in vivo* tests using nerve agent surrogates that leave AChE inhibited with the same chemical moiety as sarin or VX (Chambers *et al.*, 2013, 2016a; Meek *et al.*, 2012; Pringle *et al.*, 2018). Some of these novel oximes also produced higher survival rates and provided quicker attenuation of seizure-like behavior than 2-PAM following challenges with lethal levels of nerve agent surrogates and paraoxon (PXN) (Chambers *et al.*, 2016b). Novel Oxime 20 also prevented accumulation of the astrogliosis marker glial fibrillary acidic protein (GFAP) whereas 2-PAM did not (Pringle *et al.*, 2018).

To further study the therapeutic potential of our current 3 lead oximes, the present research was designed to examine neural damage induced by OPs and explore the ability of the novel oximes to attenuate this damage. This work measured the sparing of neuronal injury in the brains of rats challenged with the sarin surrogate, nitrophenyl isopropyl methylphosphonate (NIMP), or the insecticide metabolite, PXN, to those of rats that were similarly challenged but subsequently treated with one of our novel oximes or 2-PAM. Neuropathology was measured using NeuN, Nissl, and Fluoro-Jade B histochemical techniques. In addition, a pharmacokinetic study of the 3 oximes was conducted to describe the residence time of the oximes in the blood following IM administration. This is the first report of the protection of neurons provided by our novel oximes.

MATERIALS AND METHODS

Organophosphates and Oximes

The OPs NIMP and PXN were synthesized by the late Dr Howard Chambers using methods previously described (Meek *et al.*, 2012). 2-PAM was purchased from Sigma Aldrich (St. Louis, Missouri). The 3 novel oximes, as mesylate salts, were originally synthesized by Dr Howard Chambers and were used for the neuroprotection studies conducted at Mississippi State University, and subsequently these oximes were synthesized by chemists at SRI International using similar methods and were used for the pharmacokinetic studies conducted at SRI. Purity of all oximes was at least 95%. Structures of the 3 novel oximes are shown in Figure 1.

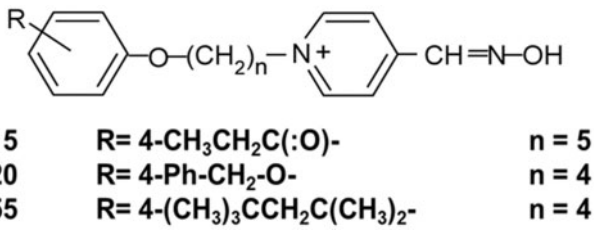

Figure 1. Structure of novel substituted phenoxyalkyl pyridinium oximes where *n* is the number of C's in the alkyl chain and R is the substitution on the phenoxy moiety.

Animal Treatment for Neuropathology

Adult male (250–300g) Sprague Dawley-derived rats from Envigo Laboratories (Prattville, Alabama) were administered SC either a lethal dosage of the sarin surrogate NIMP (0.6 mg/kg), a lethal dosage of PXN (0.8 mg/kg), or the biocompatible vehicle (Multisol: 48.5% water, 40% propylene glycol, 10% ethanol, 1.5% benzyl alcohol). At the time of initial seizure-like behavior (about 30-min post-OP exposure), rats were administered 146 μmol/kg of a novel oxime or 2-PAM in vehicle (Multisol) IM, the human equivalent dosage (HED) of 3 auto-injectors. Atropine sulfate in saline was also administered IM at a dosage of 0.65 mg/kg at this time to all OP challenged rats. Over the next 4 h, rats were administered up to 2 additional injections of atropine as necessary for control of peripheral cholinergic signs with most rats receiving 3 injections total. Rats were monitored for 8 h following the initial injection and showed similar seizure-like behavior as reported earlier (Chambers *et al.*, 2016b) and were maintained by animal facility staff for 4 days post-treatment. These procedures were performed under a protocol approved by the Mississippi State University Institutional Animal Care and Use Committee.

Perfusion

Four days after treatment, rats were perfused by a protocol adapted from Gage *et al.* (2012). The rats were deeply anesthetized with isoflurane and transcardially perfused with 0.9% sodium chloride followed by 200 ml 4% paraformaldehyde.

Processing of Perfused Rat Brains

The processing and staining techniques were modifications of existing protocols (Forster *et al.*, 2008; Pringle *et al.*, 2008). After perfusion, the rat skulls were skinned and placed into 4% paraformaldehyde for 24 h. Brains were then removed from the skulls and placed into 8 ml of 25% sucrose dissolved in phosphate-buffered saline (PBS) (0.1 M sodium phosphate, 0.16 M sodium chloride, pH 7.4) where they stayed for 4 days at 4°C to protect the architecture of the tissue during freezing. Brains were next cut in half sagittally, and the right hemisphere was flash frozen for 45–60 s in 20–25 ml of isopentane

(2-methylbutane) frozen over dry ice. Following removal from the isopentane, each hemisphere was wrapped in aluminum foil and stored at −80°C until sectioning. A total of 98 rats were challenged, perfused after 4 days, and had tissues prepared for NeuN staining. Sections from 81 of these same brains were also Nissl stained. A total of 588 sections were stained with NeuN and 486 with Nissl. Eight to 10 sections were also collected from 83 of these same brains for Fluoro-Jade staining.

NeuN and Nissl Immunofluorescent Staining

Neural damage was evaluated in the hippocampus, an area known to be involved in memory (Bannerman *et al.*, 2012) and status epilepticus (Sato and Woolley, 2016), and documented as damaged by sarin (Spradling *et al.*, 2011). A Leica Microm HM560 cryostat at around −10°C was used to slice coronal 25 μm sections from bregma −4.52 to −6.30 mm according to Paxinos and Watson (2006). Single sections were placed into individual wells of a 24-well tissue culture plate on ice, using 1 six-well row for each brain. One tissue culture plate was used for NeuN and one for Nissl and 6 sections were collected for each staining method, alternating sections between plates. Each well contained 500 μl of pre-chilled PBS, 0.01 M for NeuN staining, or 0.1 M for Nissl. For both stains, a free-floating procedure was used with a 300 μl solution volume for each change.

For neuronal nuclei (NeuN) staining, NeuN (D4G4O) XP Rabbit mAb no. 24307 from Cell Signaling Technology, Inc. (Danvers, Massachusetts) was used as the primary antibody and Goat Anti-Rabbit IgG, DyLight 488 from Pierce Biotechnology by Thermo Fisher Scientific as the fluorescent secondary.

The sections were first incubated for 2 h at room temperature on a horizontal shaker/rocker in a blocking solution comprised of 15 μl undiluted goat serum per 1 ml of diluent. The diluent already contained 1 μl undiluted goat serum for every 2.5 ml of 0.01 M PBS so the final concentration of goat serum in the blocking solution was approximately 1.5%. The blocking solution was replaced with a 1:1000 dilution of the primary antibody in diluent plus 0.2% Triton-X 100. The plate was incubated overnight at 4°C on the horizontal shaker for around 20 h while protected from light. In the morning, the plate was allowed to warm up on the shaker at room temperature in the dark for 1 h prior to removal of the primary antibody. The sections were then washed 3 times using room temperature diluent separated by 10–15 min of room temperature shaking while protected from light. Next the diluent was replaced with a 1:800 dilution of DyLight 488 plus 0.1% Triton-X 100 in diluent. The plate was shaken in the dark at room temperature for 2 h. The sections were then washed 3 times using room temperature diluent separated by 10–15 min of room temperature shaking while protected from light. After the last wash, the plate was incubated at 4°C for at least 15–20 min prior to mounting sections to slides.

For the Nissl staining, NeuroTrace 435/455 blue fluorescent Nissl stain from Invitrogen by Thermo Fisher Scientific was diluted 1:200 and used following the manufacturer's instructions. The overnight 4°C option on an orbital shaker in the dark was chosen for the final wash step.

Sections from both staining methods were mounted to Thermo Fisher Scientific Tissue Path Superfrost Plus Gold Slides that had been pretreated to promote frozen tissue adhesion. Each slide contained all the NeuN or Nissl sections from a particular rat brain, ie, 1 six-well row of the tissue culture plate. After drying, DPX-mounting media (Millipore Sigma, St. Louis, Missouri) was used prior to cover slipping. After an additional 20–30 min of drying, the slides were stored at 4°C for 24–48 h prior to imaging and scoring.

Fluoro-Jade B Immunofluorescent Staining

The brains were sectioned on the Leica Microm HM560 cryostat as described above with 25 μm sections taken 200 μm apart beginning approximately 1.5 mm anterior to the bregma and ending 5 mm posterior of the bregma according to Paxinos and Watson (2006). These sections were mounted onto gelatin-coated slides and dried overnight at room temperature. The next day the prepared slides were rehydrated in Millipore Super-Q water for 5 min prior to staining. The slides were then immersed in 0.06% potassium permanganate for 20 min on the shaker to decrease background staining and fading of the stain from either age or exposure to light (Schmued *et al.*, 1997). Slides were rinsed 3 times for 1 min each in Millipore Super-Q ultrapure water then placed in a Fluoro-Jade B/DAPI solution for 30 min while protected from light on the shaker. This solution was created by mixing 7 ml of 0.01% Fluoro-Jade B (Histo-Chem Inc., Jefferson, Arkansas) and 3 ml of 0.01% DAPI (Thermo Scientific, Rockford, Illinois) into 165 ml of 0.1% acetic acid (Schmued and Hopkins, 2000). Slides were again rinsed 3 times for 1 min each in DI water, then dehydrated by 3-min sequential immersions in 70%, 90%, and 100% ethanol solutions. This was followed by 5 min in xylene to clear sections for mounting. DPX-mounting media was used to coverslip the slides. Slides were then air dried in the dark and stored at 4°C until imaging.

Pharmacokinetic Analysis of Oximes

Following standardized methods conducted at SRI International, adult male Sprague Dawley rats from Charles River Laboratories (Hollister, California) (242–281 g; 8–9 weeks of age) were administered 1 of the 3 novel oximes IM (50 mg/kg). Animals were assigned randomly to treatment groups and singly jugular vein catheterized. Administration was no more than 0.2 ml per hind leg site; total dose volume was divided over 2 sites, one in each thigh (~ ½ volume to each hind thigh muscle). Dose volume was 1 ml/kg calculated from the body weights of each animal on the day of administration. Multisol was used for IM administration to match the vehicle and route used in the oxime efficacy studies. All injection solutions were prepared aseptically. The dose formulations were clear solutions and were prepared on the day the experiment was initiated, and they were maintained at 37°C during the time of administration. Rats were periodically observed for behavioral changes.

Blood (about 0.3 ml per sample) was collected from the jugular vein catheter at 5, 15, 30, and 45 min, and 1, 2, 4, 12, and 24 h post-dose into K_3EDTA, with 3 animals per dose group. The plasma was obtained by centrifugation, frozen at −60°C, and subsequently analyzed for the appropriate oxime by an HPLC/MS bioanalytical method developed and optimized for these oximes using acetonitrile followed by centrifugation to precipitate and remove proteins. Oxime 20 served as the internal standard for Oximes 15 and 55, and Oxime 15 served as the internal standard for Oxime 20. Gradient HPLC was conducted using mobile phase A (0.1% formic acid in water) and mobile phase B (0.1% formic acid in acetonitrile), moving from a ratio of 80%A/20%B to 10%A/90%B back to 80%A/20%B over a 4-min run time. A Phenomenex Luna C18 column was used in a Shimadzu CBM-20A system controller with Shimadzu LC-20AD pumps. MS was conducted in an API Sciex 4000 (AB Sciex) mass spectrometer, using a Turbo spray in positive ion mode and detection with

multiple reaction monitoring (MRM). Integration and quantitation were by AB Sciex Analyst Software. The lower limit of quantitation (LLOQ) was 20 ng/ml.

Data Quantification

NeuN and Nissl

NeuN and Nissl stained slides were examined using an Olympus BX60 microscope with an Infinity3 integrated camera (Lumenera Corp., Ottawa, Ontario) and an Olympus U-MWB blue 450–480 nm excitation filter to induce light emission. Images were taken of the CA1 hippocampal regions of the sections at 20× and 40× magnification. Because there has been some controversy over whether NeuN staining varies with changes in physiology (Duan *et al.*, 2016), the sections were scored for neurodegeneration using a 0–3 numerical scale. A score of 0 was given for no damage (no difference from that which is seen in known control rats), 1 for mild damage (slight shape changes), 2 for moderate damage (cells are no longer in the same plane, contain black spots and appear granular), and 3 for severe damage (numerous ablations in the CA1 region). Each slide was given a cumulative score after examining all of the sections on it. One of 2 scorers was randomly assigned the slides to score and was always blinded to the challenge which the rat had received but was knowledgeable of the staining method used on the sections. Counts were compiled into Excel for analysis.

Six to 14 individual rats were analyzed for each treatment with most treatments having less than 10. Damage percentages were calculated for each treatment group.

Due to the small sample size and the fact that several of the groups failed the ANOVA requirement of constant variance, the Kruskal-Wallis nonparametric 1-way ANOVA was used to test for significant differences among the treatment groups at $p < .05$. When the Kruskal-Wallis test found a statistically significant difference, the Mann-Whitney *U* test was used to determine which pairs of groups differed and was followed by the Benjamini-Hochberg procedure to adjust for multiple comparisons (Benjamini and Hochberg, 1995).

Fluoro-Jade B

Slides were examined, and images taken at 40× magnification using the same camera and filter as for the Nissl and NeuN slides. Three images were taken from both the hilus and CA1 regions of the hippocampus. This was done for each rat brain from the 4-day treatment group.

Fluoro-Jade B positive staining cells, indicating apoptotic or necrotic neurons, were counted in each of the images and compiled into an Excel spreadsheet for data analysis. All samples were scored by 1 counter who was blinded to their treatment. ImageJ software (from NIH) was used to assist in counting images containing high numbers of Fluoro-Jade B positive cells (Schneider *et al.*, 2012) and the Freeman-Halton extension of the Fisher exact probability test used to evaluate statistical significance.

Pharmacokinetics

The plasma drug level data were analyzed using Phoenix WinNonlin (version 6.4) software to perform noncompartmental data analysis. The dose administered was input to the program as mg/kg; therefore, no additional corrections for individual body weights of the animals were necessary.

The following parameters and constants were determined: time to maximum plasma concentration after IM dose (T_{max}), maximal plasma concentration after IM dose (C_{max}), terminal elimination half-life ($t_{1/2}$), area under the plasma concentration-time curve to the last time point (AUC_{last}) and extrapolated to infinity (AUC_{inf}), plus mean residence time to the last time point (MRT_{last}) and extrapolated to infinity (MRT_{inf}).

RESULTS

NeuN and Nissl

The NeuN sections were highly reproducible, showing the same damage percentages for each treatment regardless of OP or the number of animals used. The Nissl sections, however, showed a wide range of damage percentages (Table 1). In the NeuN sections, treatment with either OP plus 2-PAM or Oxime 15 resulted in higher damage percentages than did the OP alone.

Statistically significant differences were seen in the median damage scores between the control (vehicle) group and the groups treated with an OP (NIMP or PXN) alone ($p = .001$), OP followed by 2-PAM ($p = .0003$ for NIMP, $p = .00001$ for PXN), and OP followed by Oxime 15 ($p = .002$). Although the groups challenged with an OP followed by novel oxime 20 or 55 had somewhat higher average damage scores than the control group, the difference was not statistically significant with $p = .13$ for Oxime 55 and $p = .3$ for Oxime 20 (Figure 2). After intergroup statistical analysis with adjustment for multiple comparisons, the NIMP and 2-PAM group was statistically different from the NIMP and Oxime 20 group ($p = .01$) and the PXN and 2-PAM group was statistically different from the PXN and Oxime 55 group ($p = .006$). No other treatment group comparisons rose to the level of statistical significance. Representative photomicrographs of NeuN stained sections are shown in Figure 3.

NIMP followed by 2-PAM showed significantly more damage than NIMP followed by Oxime 20 ($p = .01$) and PXN followed by 2-PAM had greater damage than PXN followed by Oxime 55 ($p = .006$).

For the sections stained with Nissl, there were no statistically significant differences after applying the Benjamini-Hochberg correction (Figure 2).

Fluoro-Jade B

Although all exhibited seizure-like behaviors, the only rats that displayed significant Fluoro-Jade B staining for neurodegeneration were in the NIMP, PXN, and PXN followed by 2-PAM treatment groups. The number of animals that displayed neurodegeneration are shown in Table 2. None of the groups were statistically significantly different from each other with $p = .8$ for the NIMP and $p = .6$ for the PXN groups. No damage was observed when NIMP exposure was followed by oxime treatment of any type, either novel or 2-PAM. PXN damage, however, was not observed following treatment by Oximes 15 and 20; 2-PAM was ineffective in protecting against PXN.

Table 3 details the counts by region and section of the animals that showed Fluoro-Jade B staining. NIMP exposure caused greater damage to the CA1 hippocampal region than did PXN, but this was not the case in the hilus area where equivalent damage was observed. Once again, no damage was observed following NIMP challenge and treatment by any oxime, whereas no damage was observed following Oximes 15 and 20 after PXN challenge.

Pharmacokinetics

Plasma drug concentrations after administration of 50 mg/kg by IM route are shown in Table 4. One rat that was administered

Table 1. NeuN and Nissl Data From Brains of Rats Challenged With Either Nitrophenyl Isopropyl Methyl Phosphonate (NIMP) 0.6 mg/kg or Paraoxon (PXN) 0.8 mg/kg Subcutaneously With Some Receiving Pralidoxime (2-PAM), Oxime 15 (OX 15), Oxime 20 (OX 20), or Oxime 55 (OX 55)

NeuN				NISSL			
Treatment	Total Brains	Damaged Brains	Percent Damaged	Treatment	Total Brains	Damaged Brains	Percent Damaged
NIMP	12	9	75	NIMP	9	5	56
PXN	12	9	75	PXN	9	4	44
NIMP 2-PAM	7	7	100	NIMP 2-PAM	6	4	67
PXN 2-PAM	11	11	100	PXN 2-PAM	7	4	57
NIMP OX 15	7	6	86	NIMP OX 15	7	6	86
PXN OX 15	7	6	86	PXN OX 15	6	3	50
NIMP OX 20	7	2	29	NIMP OX 20	6	1	17
PXN OX 20	7	2	29	PXN OX 20	6	0	0
NIMP OX 55	7	3	43	NIMP OX 55	7	5	71
PXN OX 55	7	3	43	PXN OX 55	7	5	71
CONTROL	14	0	0	CONTROL	11	1	9

Control animals received Multisol. Rats were perfused at the 4-day time point and brains were stained with NeuN or Nissl. Included are the total number of brains in each treatment group, number of these brains that showed hippocampal damage, and this number expressed as a percentage.

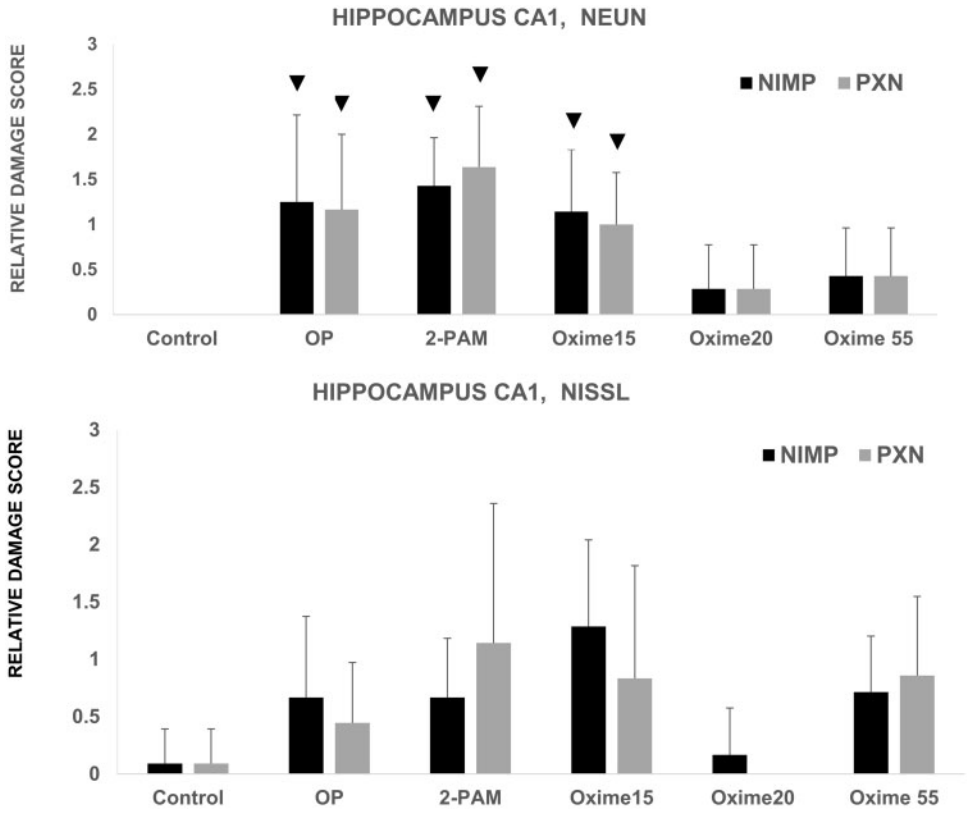

Figure 2. Relative neuropathology observed in the CA1 region of rats challenged subcutaneously with organophosphates (OP) (either nitrophenyl isopropyl methyl phosphonate [NIMP] at 0.6 mg/kg or paraoxon [PXN] at 0.8 mg/kg) with some later receiving pralidoxime (2-PAM), Oxime 15, Oxime 20, or Oxime 55. Control animals received Multisol. Sequential CA1 hippocampal sections from the same rat were stained with NeuN or Nissl. For NeuN, *n* was from 7 to 14. For Nissl, *n* was from 6 to 11. The symbol ▼ indicates a statistically significant difference between the median of this group and that of the control group; bars reflect SD. (For Nissl PXN-Oxime 20 group, all observations were 0, so no SD was calculated.)

Oxime 15 had concentrations much lower than the other rats and was considered an outlier; data from this rat were not included in additional calculations. Plasma concentrations were <LLOQ by 24 h in rats that received Oxime 15, whereas Oxime 20 and 55 treated rats had quantifiable concentrations of the test articles in the plasma through 24 h. Patterns of plasma concentrations are shown in Figure 4.

DISCUSSION

By controlling OP-induced seizure activity from ACh accumulation, antidotes should prevent neuropathology from persistent and recurrent seizures (Baille *et al.*, 2005; Chapman *et al.*, 2006; McDonough *et al.*, 1995; Shih *et al.*, 2003). Control of OP-induced seizures is critical in the prevention of neuropathology, as

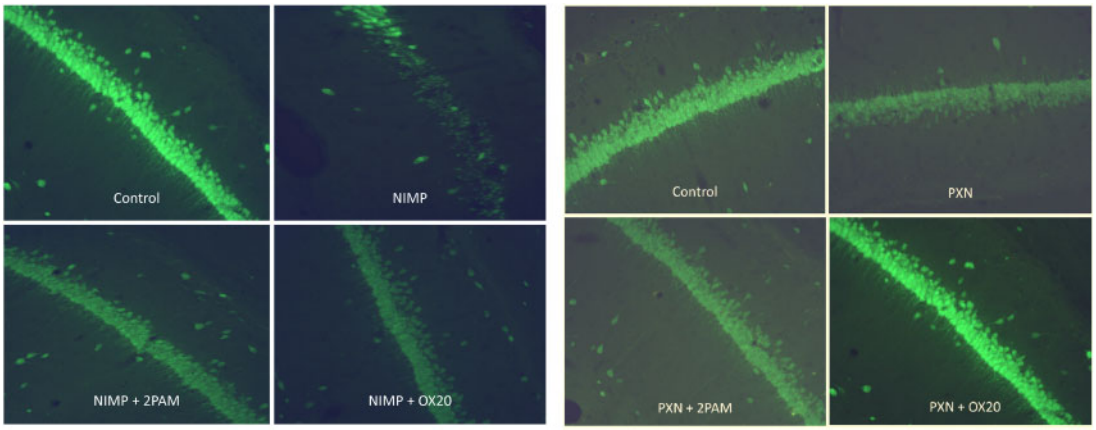

Figure 3. Representative sections of the CA1 hippocampal regions from rats challenged subcutaneously with either nitrophenyl isopropyl methyl phosphonate (NIMP) at 0.6 mg/kg or paraoxon (PXN) at 0.8 mg/kg with some receiving Oxime 20 (OX20) or pralidoxime (2-PAM). Control animals received Multisol. Rats were perfused at the 4-day time point and brains were stained with NeuN. Photomicrographs are at 20× magnification.

Table 2. Fluoro-Jade B Data From Brains of Rats Challenged With Either Nitrophenyl Isopropyl Methyl Phosphonate (NIMP) 0.6 mg/kg or Paraoxon (PXN) 0.8 mg/kg Subcutaneously With Some Receiving Oxime 15 (OX 15), Oxime 20 (OX 20), or Pralidoxime (2-PAM)

	NIMP	NIMP 2-PAM	NIMP OX 15	NIMP OX 20	PXN	PXN 2-PAM	PXN OX 15	PXN OX 20	Control
Total brains	15	6	7	6	13	12	6	7	11
Damaged brains	2	0	0	0	2	2	0	0	0
Percent damaged	13	0	0	0	15	17	0	0	0

Control animals received Multisol. Rats were perfused at the 4-day time point and brains were stained with Fluoro-Jade B. Included are the total number of brains in each treatment group, number of these brains that showed hippocampal damage, and this number expressed as a percentage.

Table 3. Regional Fluoro-Jade B Data From Brains of Rats Challenged With Either Nitrophenyl Isopropyl Methyl Phosphonate (NIMP) 0.6 mg/kg or Paraoxon (PXN) 0.8 mg/kg Subcutaneously With Some Receiving Oxime 15 (OX 15), Oxime 20 (OX 20), or pralidoxime (2-PAM)

Dying Neurons by Region	Control	NIMP	NIMP 2-PAM	NIMP Oxime 15	NIMP Oxime 20	PXN	PXN 2-PAM	PXN Oxime 15	PXN Oxime 20
CA1	1	340	1	1	1	70	49	0	2
Hilus	1	199	1	1	0	261	208	0	3
Total brains	11	15	6	6	7	13	12	7	6

Control animals received Multisol. Rats were perfused at the 4-day time point and brains were stained with Fluoro-Jade B. The total number of dying neurons per region are shown.

persistent seizure activity from the accumulation of ACh and glutamate is strongly associated with brain damage (Baille *et al.*, 2005; McDonough *et al.*, 1995). The examination of excitotoxic neurodegeneration is an important aspect of the investigation of both the OP exposure models used here and the novel pyridinium oximes developed for the treatment of OP intoxication. Neurodegeneration is a well-documented outcome of CWA exposure, and neuronal damage has been linked to behavioral alterations and cognitive impairment (Myhrer *et al.*, 2005). Recent work has also shown that cholinergic neuromodulation in the hippocampus is critical to context memory formation and that errors here can lead to fear behaviors similar to those seen in PTSD patients, like those of the Tokyo attack (Raza *et al.*, 2017).

With NeuN in the present study, rats challenged with NIMP or PXN followed by Oximes 20 or 55 had damage levels that were not different statistically from the vehicle controls. The p values seen for the comparisons between controls and OPs followed by Oxime 20 ($p = .3$) or Oxime 55 ($p = .1$) indicate a lack of statistical difference amongst these groups. This indicates that Oximes 20 and 55 kept OP damage low enough as to not be statistically different from that seen in the controls.

NeuN-stained sections were much easier to score for neuropathology because they were clear enough to identify individual neurons (Figure 3). Nissl staining yielded a much less distinct aspect in which it was difficult to discern individual cells. Because the clarity and definition of NeuN was greater than Nissl, it was much easier to see differences among NeuN-stained sections than those stained with Nissl. We suspect that this is the reason for the lack of statistical significance seen among the Nissl-stained sections in Figure 2 and the large variability of the Nissl damage percentages in Table 1. However, Figure 2 shows that the pattern of Nissl results were generally consistent with the NeuN results.

These results indicated that neuroprotection was afforded to both the sarin surrogate (NIMP) and the OP insecticide metabolite (PXN) by Oxime 20, which strongly suggested that it penetrated the BBB. The NeuN results also suggested that Oxime 55 likewise penetrated the BBB and afforded protection against NIMP and PXN (Figure 2). Oxime 15, however, did not afford neuroprotection in this study.

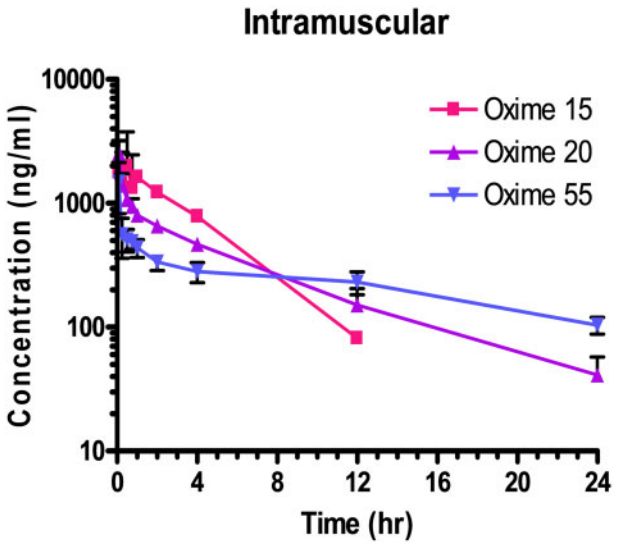

Figure 4. Male Sprague Dawley rats received a single dose of Oxime 15, 20, or 55 by IM (50 mg/kg) injection. Each data point represents the mean ± SD of $n = 3$ rats, except for the IM dose of Oxime 15 in which one rat was considered an outlier and data from this animal were not included in additional calculations. Samples collected prior to dose administration were <lower limit of quantitation.

Because the rats challenged with NIMP or PXN followed by 2-PAM had damage levels that were not statistically different from NIMP or PXN alone but were statistically different from the controls, this indicates that 2-PAM is not capable of protecting against neurodegeneration, as expected. This assertion is also supported by the fact that the NIMP and Oxime 20 and PXN and Oxime 55 groups had statistically lower damage scores than their corresponding OP and 2-PAM groups.

The damage percentages of the NeuN sections also lend credence to the idea that 2-PAM and Oxime 15 failed to provide neuroprotection because their values of 100% and 85.7% respectively were higher than that seen for treatment with either OP alone (75%).

For measurement of neurodegeneration, Fluoro-Jade B provides a specific measure of dying neurons (Schmued *et al.*, 1997; Schmued and Hopkins, 2000). This stain has been previously used in other animal model studies of nerve agent exposure (Myhrer *et al.*, 2005, 2006). As this stain is not selective for either necrotic or apoptotic processes, it provides a measure of total dying neurons, which are seen to display varying degrees of necrotic and apoptotic properties (Baille *et al.*, 2005). As not all neurons that will die from OP intoxication do so immediately, Fluoro-Jade B staining should give a measure of the degree of neuronal death that is expected to occur but has not yet been completed.

The results of the 4-day time point demonstrated that lethal doses of both NIMP and PXN are capable of producing Fluoro-Jade B measured neurodegeneration in the rat model of OP exposure but not at the level previously reported in the literature. Previous work (McDonough *et al.*, 1995) which used male Sprague Dawley rats treated with soman SC at 0.18 mg/kg produced neurodegeneration in 98% of animals treated, whereas the NIMP treatment in the present study produced neurodegeneration in only 13% of treated animals at the 4-day time point. Although a highly relevant surrogate of sarin, signs of severe poisoning occur slower with NIMP (about 30 min) than sarin (a few min, as reported in the literature), and this slower action with NIMP may have provided a higher proportion of the animals an opportunity to adapt than is possible with the very rapid action of sarin. No rat administered NIMP followed by any of the 4 oximes studied showed any sign of neurodegeneration as indicated by Fluoro-Jade B staining.

PXN has been shown to produce neurodegeneration with dosages ranging from 0.45 to 4 mg/kg (Deshpande *et al.*, 2016; Finkelstein *et al.*, 2012; Krishnan *et al.*, 2016). Deshpande *et al.* (2014) examined dosages from 0.1 to 8 mg/kg of PXN alone in male Sprague Dawley rats. At the dose used in the present work (0.8 mg/kg), they observed 71% of treated animals undergoing status epilepticus with a mortality rate of 50%. Following PXN exposure in the present work, 15% of rats displayed significant neurodegeneration. Rats challenged with PXN and treated with 2-PAM displayed neurodegeneration at essentially the same rate (17%) yet none of the rats challenged with PXN and treated with Oxime 15 or 20 displayed significant neurodegeneration (Table 2).

Although rats treated with kainic acid displayed significant neurodegeneration at 4 days, verifying that the Fluoro-Jade B staining method we used properly labeled degenerate neurons, we did not see the high proportion of Fluoro-Jade staining with PXN and other OPs reported by other authors. This may be due to the 4-day time point that we used. Both Anderson *et al.* (2005) and Wang *et al.* (2008) found that peak levels of Fluoro-Jade B and C staining occurred at 3 days or less. It is possible that because Fluoro-Jade provides a specific measure of dying neurons and measures the degree of neuronal death that is expected to occur but has not yet been completed (Schmued *et al.*, 1997; Schmued and Hopkins, 2000), that the reason little Fluoro-Jade staining was observed was that most neuronal death had already happened by the 4-day time point. Perhaps some OPs require the use of an earlier time point than kainic acid. Our use of a Fluoro-Jade B/DAPI mixture may also have contributed to the low levels of staining. Ehara and Ueda (2009) noted that it is unclear whether one should stain with Fluoro-Jade first or second in double-labeling attempts and that the method varies widely but it appears that most labs separate the 2 steps instead of using a mixture of the 2.

In addition, we had better results with the NeuN and Nissl stains which used a free-floating method rather than the slide mounted one we used for Fluoro-Jade. Recent work (Gutiérrez *et al.*, 2018) adapted Fluoro-Jade to a free-floating method and found more intense staining with a reduction in background signal.

The low rate of damage makes it difficult to reach valid conclusions from the results and may explain the apparent NIMP protection afforded by 2-PAM, which was not observed in the NeuN or Nissl results (Table 2). The lack of statistical significance is likely partly due to the low number of damaged samples. However, we included the Fluoro-Jade data because they suggest, as did the NeuN and Nissl stains, that the novel oximes afford protection against PXN neurodegeneration whereas 2-PAM does not.

The combined results from the NeuN, Nissl, and Fluoro-Jade B staining indicate that novel Oximes 20 and possibly 55 can protect against neurodegeneration and have potential in the treatment of both OP insecticidal poisoning and nerve agent exposures. This broad spectrum of usefulness is lacking with 2-PAM. This is an encouraging result because insecticides are more frequently the agents of OP poisoning and the oximes presently in use are of limited clinical benefit (Eddleston and Chowdhury, 2016). Oximes 20 and 55 appear to be reactivators with a broad spectrum of action, which has been indicated as a definite need (Worek *et al.*, 2016).

Table 4. Pharmacokinetic Parameters for Oximes 15, 20, and 55 in Male Sprague Dawley Rats After Single Intramuscular (IM) Dose, 50 mg/kg

Oxime		T_{max} (h)	C_{max} (ng/ml)	$t_{1/2}$(h)	AUC_{last} (h·ng/ml)	AUC_{inf} (h·ng/ml)	MRT_{last} (h)	MRT_{inf} (h)
15[a]	Rat 11[a]	0.500	2230	2.79	8874	9289	3.55	3.56
	Rat 12[a]	0.500	3620	2.23	9268	9462	2.84	2.84
20	Mean	0.083	2547	5.20	6689	7006	6.50	6.39
	SD	0.000	640	0.59	945	1094	1.11	1.11
55	Mean	0.083	1227	13.8	5656	7671	18.2	18.7
	SD	0.000	654	0.31	1015	1344	0.13	0.41

[a]There were 2 replications for Oxime 15, and 3 replications for Oximes 20 and 55. For Oxime 15, 1 animal was an outlier therefore, the data from that animal were not used in further calculations. Therefore the 2 individual values for this group are shown to illustrate that there was little individual variation in the PK parameters between the 2 rats.

The positive results here with Oxime 55 were somewhat surprising in that it has previously shown the least potential for CNS protection of our 3 lead oximes, having displayed little attenuation of seizure-like behavior from these same lethal level dosages (unpublished information), whereas Oxime 20 did show appreciable attenuation (Chambers *et al.*, 2016b). This attenuation occurred within the first 6–8 h following OP challenge. The histological results reported here were for 4 days following OP challenge. The pharmacokinetics study indicated a plasma half-life following IM administration of 2.5, 5.2, and 13.8 for Oximes 15, 20, and 55, respectively (Table 4). These half-lives may be partially related to the lipophilicities of these oximes; octanol: water partition coefficients are 0.056, 0.35 and 1.46 for Oximes 15, 20 (Chambers *et al.*, 2013) and 55, respectively. The shortest plasma residence time may have been insufficient for Oxime 15 to promote significant neuroprotection whereas the longer time for Oxime 20 and especially for Oxime 55 may have been the reason that neuroprotection was observed. Oxime 55 may have been absorbed sufficiently slowly, perhaps because of its larger size, to be ineffective in attenuating the short-term seizure-like behavior in our earlier study.

Oxime 20 has been overall the most effective of our oxime platform, showing the highest level of brain AChE reactivation (35% in 2 h) (Chambers *et al.*, 2013), the best performance in attenuating seizure-like behavior (Chambers *et al.*, 2016b) and the best performance in neuroprotection (Pringle *et al.*, 2018 and the present study) so Oxime 20 remains, at present, our lead candidate.

The data in this study support that NIMP and PXN have the potential to serve as highly relevant models of nerve agent and insecticide induced neuropathology and that Oxime 20 and perhaps 55 may be able to mitigate this damage, with promise of preventing long-term cognitive sequelae. This novel platform of substituted phenoxyalkyl pyridinium oximes continues to show positive results of neuroprotection within the brain that 2-PAM cannot provide.

DECLARATION OF CONFLICTING INTERESTS

This oxime platform was patented by Mississippi State University (U.S. patent 9, 277, 937; European patents pending) and was licensed by Defender Pharmaceuticals, Inc., which had no input into the design of the experiments or the interpretation of the results.

ACKNOWLEDGMENTS

The technical assistance of Mr W. Shane Bennett at Mississippi State University is appreciated. Novel oximes are protected under U.S. Patent 9, 277, 937, owned by Mississippi State University, and patent rights have been licensed exclusively to Defender Pharmaceuticals. Inc. The laboratory assistance of Kathleen O'Loughlin, Dr Chun Yang, and Leyi Gong at SRI is appreciated.

FUNDING

National Institute of Neurological Disorders and Stroke of the National Institutes of Health (U01NS083430 and U01NS107127 to Mississippi State University) and the CounterACT Preclinical Development Facility (HHSN271200623691C to SRI). The content is solely the responsibility of the authors and does not necessarily represent the official views of the National Institutes of Health.

REFERENCES

Anderson, K. J., Miller, K. M., Fugaccia, I., and Scheff, S. W. (2005). Regional distribution of Fluoro-Jade B staining in the hippocampus following traumatic brain injury. *Exp. Neurol.* **193**, 125–130.

Aroniadou-Anderjaska, V., Figueiredo, T. H., Apland, J. P., Prager, E., Pidoplichko, V., Miller, S., and Braga, M. F. M. (2016). Long-term neuropathological and behavioral impairments after exposure to nerve agents. *Ann. N.Y. Acad. Sci.* **1374**, 17–28.

Baille, V., Clarke, P., Brochier, G., Dorandeu, F., Verna, J., Four, E., Lallement, G., and Carpentier, P. (2005). Soman-induced convulsions: The neuropathology revisited. *Toxicology* **215**, 1–24.

Bannerman, D. M., Bus, T., Taylor, A., Sanderson, D. J., Schwarz, I., Jensen, V., Hvalby, Ø., Rawlins, J. N., Seeburg, P. H., and Sprengel, R. (2012). Dissecting spatial knowledge from spatial choice by hippocampal NMDA receptor deletion. *Nat. Neurosci.* **15**, 1153–1159.

Benjamini, Y., and Hochberg, Y. (1995). Controlling the false discovery rate: A practical and powerful approach to multiple testing. *J. Roy. Stat. Soc.* **B 57**, 289–300.

Chambers, J. E., Chambers, H. W., Funck, K. E., Meek, E. C., Pringle, R. B., and Ross, M. K. (2016a). Efficacy of novel phenoxyalkyl pyridinium oximes as brain-penetrating reactivators of cholinesterase inhibited by surrogates of sarin and VX. *Chem. Biol. Interact.* **259**, 154–159.

Chambers, J. E., Chambers, H. W., Meek, E. C., and Pringle, R. B. (2013). Testing of novel brain-penetrating oxime reactivators of acetylcholinesterase inhibited by nerve agent surrogates. *Chem. Biol. Interact.* **203**, 135–138.

Chambers, J. E., Meek, E. C., Bennett, J. P., Bennett, W. S., Chambers, H. W., Leach, C. A., Pringle, R. B., and Wills, R. W. (2016b). Novel substituted phenoxyalkyl pyridinium oximes enhance survival and attenuate seizure-like behavior of rats

receiving lethal levels of nerve agent surrogates. *Toxicology* **339**, 51–57.

Chapman, S., Kadar, T., and Gilat, E. (2006). Seizure duration following sarin exposure affects neuro-inflammatory markers in the rat brain. *Neurotoxicology* **27**, 277–283.

Chen, Y. (2012). Organophosphate-induced brain damage: Mechanisms, neuropsychiatric and neurological consequences, and potential therapeutic strategies. *Neurotoxicology* **33**, 391–400.

Deshpande, L., Blair, R., Huang, B., Phillips, K., and DeLorenzo, R. (2016). Pharmacological blockade of the calcium plateau provides neuroprotection following organophosphate paraoxon induced status epilepticus in rats. *Neurotoxicol. Teratol.* **56**, 81–86.

Deshpande, L., Carter, D., Phillips, K., Blair, R., and DeLorenzo, R. (2014). Development of status epilepticus, sustained calcium elevations and neuronal injury in a rat survival model of lethal paraoxon intoxication. *Neurotoxicology* **44**, 17–26.

Duan, W., Zhang, Y., Hou, Z., Huang, C., Zhu, H., Zhang, C., and Yin, Q. (2016). Novel insights into NeuN: From neuronal marker to splicing regulator. *Mol. Neurobiol.* **53**, 1637–1647.

Eddleston, M., and Chowdhury, F. (2016). Pharmacological treatment of organophosphorus insecticide poisoning: The old and the (possible) new. *Br. J. Clin. Pharmacol.* **81**, 462–470.

Ehara, A., and Ueda, S. (2009). Application of Fluoro-Jade C in acute and chronic neurodegeneration models: Utilities and staining differences. *Acta Histochem. Cytochem.* **42**, 171–179.

Finkelstein, A., Kunis, G., Berkutzki, T., Ronen, A., Krivoy, A., Yoles, E., Last, D., Mardor, Y., Shura, K., McFarland, E., *et al.* (2012). Immunomodulation by poly-YE reduces organophosphate-induced brain damage. *Brain Behav. Immun.* **26**, 159–169.

Forster, G., Pringle, R., Mouw, N., Vuong, S., Watt, M., Burke, A., Lowry, C., Summers, C., and Renner, K. (2008). Corticotropin-releasing factor in the dorsal raphe nucleus increases medial prefrontal cortical serotonin via type 2 receptors and median raphe nucleus activity. *Eur. J. Neurosci.* **28**, 299–310.

Gage, G., Kipke, D., and Shain, W. (2012). Whole animal perfusion fixation for rodents. *J. Vis. Exp.* Jul 30; (65), pii: 3564.

Gutiérrez, I. G., González-Prieto, M., García-Bueno, B., Caso, J. R., Leza, J. C., and Madrigal, L. M. (2018). Alternative method to detect neuronal degeneration and amyloid β accumulation in free-floating brain sections with Fluoro-Jade. *ASN Neuro* **10**, 1–7.

Hay, A. (2018). Novichok: The deadly story behind the nerve agent in Sergei Skripal spy attack. *The Conversation*, 20 March. [Online] Available at: http://theconversation.com/novichok-the-deadly-story-behind-the-nerve-agent-in-sergei-skripal-spy-attack-93562. Accessed March 29, 2018.

Krishnan, J., Arun, P., Appu, A., Vijayakumar, N., Figueiredo, T., Braga, M., Baskota, S., Olsen, C., Farkas, N., Dagata, J., *et al.* (2016). Intranasal delivery of obidoxime to the brain prevents mortality and CNS damage from organophosphate poisoning. *Neurotoxicology* **53**, 64–73.

Loh, Y., Swanberg, M., Ingram, M., and Newmark, J. (2010). Case report: Long-term cognitive sequelae of sarin exposure. *Neurotoxicology* **31**, 244–246.

Loveluck, L. (2017). Autopsies point to the use of sarin. *The Washington Post*, July 4, 2017. Article Accession Number: wapo.4d660ac4-1aa7-11e7-8003-f55b4c1cfae2. https://www.highbeam.com. Accessed January 23, 2018.

McDonough, J. H., Jr, Dochterman, L., Smith, C., and Shih, T. M. (1995). Protection against nerve agent-induced neuropathology, but not cardiac pathology, is associated with the anticonvulsant action of drug treatment. *Neurotoxicology* **16**, 123–132.

Meek, E. C., Chambers, H. W., Coban, A., Funck, K. E., Pringle, R. B., Ross, M. K., and Chambers, J. E. (2012). Synthesis and *in vitro* and *in vivo* inhibition potencies of highly relevant nerve agent surrogates. *Toxicol. Sci.* **126**, 525–533.

Myhrer, T., Andersen, J., Nguyen, N., and Aas, P. (2005). Soman-induced convulsions in rats terminated with pharmacological agents after 45 min: Neuropathology and cognitive performance. *Neurotoxicology* **26**, 39–48.

Myhrer, T., Enger, S., and Aas, P. (2006). Efficacy of immediate and subsequent therapies against soman-induced seizures and lethality in rats. *Basic Clin. Pharmacol. Toxicol.* **98**, 184–191.

Paxinos, G., and Watson, C. (2006). *The Rat Brain in Stereotaxic Coordinates*, 6th ed. Academic Press, London.

Pringle, R. B., Meek, E. C., Chambers, H. W., and Chambers, J. E. (2018). Neuroprotection from organophosphate-induced damage by novel phenoxyalkyl pyridinium oximes in rat brain. *Toxicol. Sci.* **166**, 420–427.

Pringle, R. B., Mouw, N. J., Lukkes, J. L., and Forster, G. L. (2008). Amphetamine treatment increases corticotropin-releasing factor receptors in the dorsal raphe nucleus. *Neurosci. Res.* **62**, 62–65.

Raza, S. A., Albrecht, A., Çalışkan, G., Müller, B., Demiray, Y. E., Ludewig, S., Meis, S., Faber, N., Hartig, R., Schraven, B., *et al.* (2017). HIPP neurons in the dentate gyrus mediate the cholinergic modulation of background context memory salience. *Nat. Commun.* **8**, 189.

Sakurada, K., Matsubara, K., Shimizu, K., Shiono, H., Seto, Y., Tsuge, K., Yoshino, M., Sakai, I., Mukoyama, H., and Takatori, T. (2003). Pralidoxime iodide (2-PAM) penetrates across the blood-brain barrier. *Neurochem. Res.* **28**, 1401–1407.

Sato, S. M., and Woolley, C. S. (2016). Acute inhibition of neurosteroid estrogen synthesis suppresses status epilepticus in an animal model. *Elife* **5**, pii: e12917.

Schmued, L., Albertson, C., and Slikker, W. (1997). Fluoro-Jade: A novel fluorochrome for the sensitive and reliable histochemical localization of neuronal degeneration. *Brain Res.* **751**, 37–46.

Schmued, L., and Hopkins, K. (2000). Fluoro-Jade B: A high affinity fluorescent marker for the localization of neuronal degeneration. *Brain Res.* **874**, 123–130.

Schneider, C., Rasband, W., and Eliceiri, K. (2012). NIH Image to ImageJ: 25 years of image analysis. *Nat. Methods* **9**, 671–675.

Shih, T. M., Duniho, S., and McDonough, J. H., Jr (2003). Control of nerve agent-induced seizures is critical for neuroprotection and survival. *Toxicol. Appl. Pharmacol.* **188**, 69–80.

Spradling, K. D., Lumley, L. A., Robison, C. L., Meyerhoff, J. L., and Dillman, J. F. (2011). Transcriptional responses of the nerve agent-sensitive brain regions amygdala, hippocampus, piriform cortex, septum, and thalamus following exposure to the organophosphonate anticholinesterase sarin. *J. Neuroinflammation* **8**, 84.

Swenson, K. (2017). A gruesome North Korean murder plot: Trial sheds new light on assassination of Kim Jong Un's brother. *The Washington Post*, 17 October. [Online] Available at: https://www.washingtonpost.com/news/morning-mix/wp/2017/10/17/the-gruesome-nerve-agent-assassination-of-kim-jong-uns-brother/? utm_term=.16b80d46ca9d. Accessed March 29, 2018.

Wang, L., Liu, Y., Huang, Y., and Chen, L. (2008). Time-course of neuronal death in the mouse pilocarpine model of chronic

epilepsy using Fluoro-Jade C staining. *Brain Res.* **1241**, 157–167.

Watson, A., Opresko, D., Young, R., Hauschild, V., King, J., Bakshi, K. (2009). Organophosphate nerve agents. In *Handbook of Toxicology of Chemical Warfare Agents* (R. C. Gupta, Ed.), pp. 43–67. Academic Press, London.

Worek, F., Thiermann, H., and Wille, T. (2016). Oximes in organophosphate poisoning: 60 years of hope and despair. *Chem. Biol. Interact.* **259**, 93–98.

Yanagisawa, N., Morita, H., and Nakajima, T. (2006). Sarin experiences in Japan: Acute toxicity and long-term effects. *J. Neurol. Sci.* **249**, 76–85.